Edgewise vibration control of wind turbine blades using roller and liquid dampers

Z L Zhang and S R K Nielsen

Department of Civil Engineering, Aalborg University, 9000 Aalborg, Denmark

Email: zlz@civil.aau.dk

Abstract. This paper deals with the passive vibration control of edgewise vibrations by means of roller dampers and tuned liquid column dampers (TLCDs). For a rotating blade, the large centrifugal acceleration makes it possible to use roller dampers or TLCDs with rather small masses for effectively suppressing edgewise vibrations. The roller dampers are more volumetrically efficient due to the higher mass density of the steel comparing with the liquid. On the other hand, TLCDs have their advantage that it is easier to specify the optimum damping of the damper by changing the opening ratio of the orifice. In this paper, 2-DOF nonlinear models are suggested for tuning a roller damper or a TLCD attached to a rotating wind turbine blade, ignoring the coupling between the blade and the tower. The decoupled optimization is verified by incorporating the optimized damper into a more sophisticated 13-DOF wind turbine model with due consideration of the coupled blade-tower-drivetrain vibrations, quasi-static aeroelasticity as well as a collective pitch controller. Performances of the dampers are compared in terms of the control efficiency and the practical applications. The results indicate that roller dampers and TLCDs at optimal tuning can effectively suppress the dynamic response of wind turbine blades.

List of some important symbols

ω_0	1st edgewise eigenfrequency of the blade	ω_d	natural frequency of the damper
m	mass of the damper (roller or liquid column)	m_0	1st modal mass of the blade
Ω	rotational speed of the rotor	x_0	mounting position of the damper
χ	frequency ratio ω_d/ω_0	μ	mass ratio m/m_0
μ_f	coefficient of rolling friction between surfaces	η	reduction ratio of the edgewise vibration
α	cross-section ratio of the vertical column versus horizontal column	γ	ratio of the horizontal length to total length of the liquid column
ξ	head loss coefficient due to the orifice		

1. Introduction

Traditionally, the modes of vibration in wind turbine blades are classified as flap-wise and edgewise modes. Flap-wise vibrations are blade motions out of the plane of rotating rotor, whereas edgewise vibrations take place in the rotor plane. Modal damping in the flap-wise direction is relatively high due to the strong aerodynamic damping when the turbulence flow is attached to the blade [1]. In contrast, edgewise vibrations are associated with insignificant aerodynamic damping [1], which gives rise to the increased dynamic responses and fatigue damage. Moreover, the edgewise vibrations will increase the fluctuations of the generator torque and hence influence the quality of the generated power.

Structural control technologies, which have achieved significant success in mitigating vibrations in civil engineering structures, are being increasingly investigated for application in wind turbines in recent years. Most of these studies focus on the vibration control of wind turbine towers using external dampers [2-4]. Limited studies have been carried out regarding the structural control of blade vibrations. Active TMDs have been studied for mitigating edgewise vibrations in wind turbine blades, and the results show that the active TMDs achieve greater response reductions than the passive counterpart [5]. An active strut installed near the root of the blade was proposed in [6] for the control of blade vibrations, the concept of which is based on resonant interaction between the rotor and the controller. The use of active tendons mounted inside each blade is described in [7] for the active control of edgewise vibrations. The controller allows a variable control force to be applied in the edgewise direction according to a prescribed control law. However, all the above-mentioned active control solutions need relatively complicated controller configurations and some amount of power input. This indicates the importance and necessity of developing simple and robust dampers for wind turbine blades.

In the present paper, roller dampers and tuned liquid column dampers (TLCD) are proposed for passive control of edgewise vibrations in wind turbine blades. In the case of building or tower vibrations, the oscillations of the roller or the liquid column, and hence the control effect of the roller damper or the TLCD are governed by the gravitational acceleration g. For the rotating blade the corresponding control effect is governed by the centrifugal acceleration, which can reach to a magnitude of 7-8 g for the outboard of a 65 m-long blade. This makes it possible to use roller dampers or TLCDs with rather small masses for effectively suppressing edgewise vibrations. Reduced 2-DOF nonlinear models are established for a rotating blade mounted with a roller damper or a TLCD. The turning and parametric studies of the dampers are carried out based on the decoupled 2-DOF models, with the modal loads obtained from a more sophisticated 13-DOF aeroelastic wind turbine model [8] subjected to a 3-dimensinal turbulence field. The performances of the optimized dampers are analyzed and compared.

2. Equations of motion of the blade-damper system

Since the focus is on studying the interaction between the damper and the blade and the control effect of the damper on edgewise vibrations, the coupling between the blade with the tower and the drivetrain are ignored in the following formulation. Hence, only edgewise blade vibrations are considered, and the design of the damper is totally based on the local dynamics of the rotating blade.

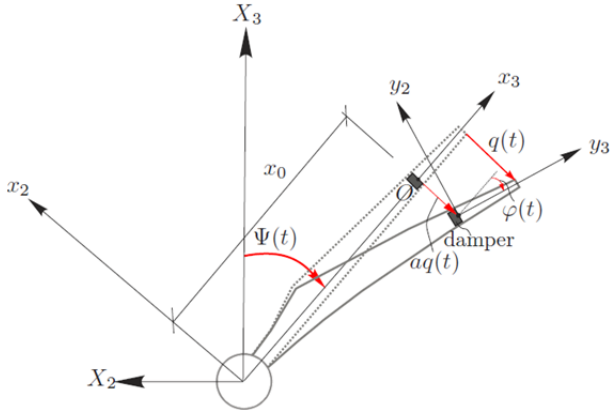

Figure 1: Definition of coordinate system, geometry and degrees of freedom

Figure 1 shows the schematic representation of a rotating blade equipped with a roller damper or a TLCD. The edgewise vibration of the blade is described in the moving local (x_2, x_3)- coordinate system, while the motion of the damper inside the deformed blade is described in another local coordinate system (y_2, y_3) fixed to the damper. The mass per unit length and the bending stiffness in the edgewise direction of each blade are denoted $\mu(x_3)$ and $EI(x_3)$, respectively. The damper is merely

devised to control the fundamental edgewise mode described by the degree of freedom $q(t)$. Then, the local edgewise displacement $u_2(x_3, t)$ of the rotating blade in the x_2- direction can be described as $u_2(x_3,t) = -\Phi(x_3)q(t)$, where $\Phi(x_3)$ indicated the fundamental eigenmode of the edgewise vibration. This is normalized to 1 at the tip, i.e. $\Phi(L_b)=1$, where L_b denotes the blade length. The rotation of the blade is assumed to take place with a constant rotational speed Ω.

It is assumed that the damper is placed at the coordinate $x_3=x_0$ inside the blade. Hence the local displacement and rotation of the blade at this position with the sign definitions in Figure 1 are given as:

$$u_{2,d}(t) = -aq(t), \quad \varphi(t) = bq(t) \tag{1}$$

where the auxiliary parameters are introduced: $a = \Phi(x_0)$, $b = \frac{d}{dx_3}\Phi(x_3)\,|_{x_3=x_0}$.

The velocity components of the blade in the moving (x_2, x_3)- coordinate system can be written as:

$$\left.\begin{aligned} v_{2,b}(x_3,t) &= -\Omega x_3 - \Phi(x_3)\dot{q}(t) \\ v_{3,b}(x_3,t) &= -\Omega\Phi(x_3)q(t) \end{aligned}\right\} \tag{2}$$

Hence, the kinetic and potential energy of the blade without damper becomes:

$$\begin{aligned} T_b &= \frac{1}{2}m_0(\dot{q}^2 + \Omega^2 q^2) + m_2\Omega\dot{q} + \frac{1}{2}\Omega^2 m_3 \\ U_b &= \frac{1}{2}k_0 q^2 = \frac{1}{2}(k_e + k_1\Omega^2 - k_2 g\cos(\Omega t))q^2 \end{aligned} \tag{3}$$

where $m_0 = \int_0^L \mu(x_3)\Phi^2(x_3)dx_3$, $m_1 = \int_0^L \mu(x_3)x_3\Phi(x_3)dx_3$, $m_2 = \int_0^L \mu(x_3){x_3}^2 dx_3$. $k_e = \int_0^L EI(x_3)\left(\frac{d^2\Phi(x_3)}{dx_3^2}\right)^2 dx_3$ is the elastic stiffness of the blade without geometric contributions. The term $k_1\Omega^2$ indicates the geometrical stiffening due to the centrifugal acceleration, and the term $k_2 g\cos(\Omega t)$ indicates the geometrical softening cause by the variation of the axial force during rotating due to the weight of the blade, where $k_1 = \int_0^L \left(\int_{x_3}^L \mu(\xi)\xi d\xi\right)\left(\frac{d\Phi(x_3)}{dx_3}\right)^2 dx_3$, $k_2 = \int_0^L \left(\int_{x_3}^L \mu(\xi)d\xi\right)\left(\frac{d\Phi(x_3)}{dx_3}\right)^2 dx_3$.

The fundamental edgewise angular eigenfrequency of the blade when it is in stand still position can be obtained as:

$$\omega_0 = \sqrt{k_e / m_0} \tag{4}$$

2.1. Roller damper

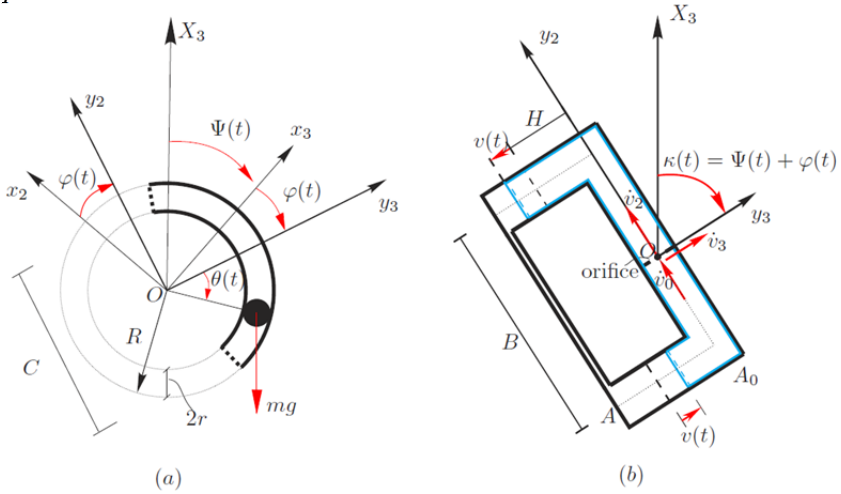

Figure 2: Geometry of the dampers. (a) roller damper, (b) TLCD

As shown in Figure 2 (a), the roller damper consists of a ball with a mass of *m* rolling back and forth inside a circular tube. By tuning the natural frequency of the roller to the 1st edgewise eigenfrequency of the blade, the damper could effectively absorb energy from the 1st edgewise mode and thus add damping to the system. The radius of the roller and the outer radius of the tube are denoted *r* and *R*, respectively. Depending on the available space inside the hollow blade, the tube may be devised in the form of a complete circle or an arc. The position of the roller inside the tube is defined by the clockwise rotation $\theta(t)$ from y_3-axis. Hence, $q(t)$ and $\theta(t)$ make up the degrees of freedom of the blade-damper system. The potential and kinetic energy of the roller can be written as:

$$U_d = mg\left(x_0 \cos\Psi - aq\sin\Psi + R_e\cos(\Psi + bq + \theta)\right) \tag{5}$$

$$T_d = \frac{1}{2}m_e\left[(x_0\Omega + a\dot{q})^2 + a^2q^2\Omega^2 + R_e^2(\Omega + b\dot{q} + \dot{\theta}) + 2R_e(\Omega + b\dot{q} + \dot{\theta})\left((x_0\Omega + a\dot{q})\cos(bq+\theta) + aq\Omega\sin(bq+\theta)\right)\right] \tag{6}$$

where $m_e = (7/5)m$, $R_e = R - r$ are the equivalent mass and equivalent length, respectively [8].

As the damper mass rolls along the tube, a friction force $f(t)$ takes place due to the rolling friction between the contacting surfaces, the magnitude of which is proportional to the normal force acting on the roller through the tube. In a rotating blade, this normal force is governed by the centrifugal force since it is much larger than the gravity force. The friction force can be given by:

$$f(t) = \mu_f[mR_e\dot{\theta}^2 + mx_0\Omega^2\cos(bq+\theta)]\mathrm{sign}(\dot{\theta}) \tag{7}$$

where μ_f is the coefficient of rolling friction between the surfaces. Then, the two generalized loads for the degrees of freedom $q(t)$ and $\theta(t)$ are given by:

$$F_q(t) = f_0(\dot{q},t) - c_0\dot{q}, \quad F_\theta(t) = -R_e f(t) = -\mu_f R_e[mR_e\dot{\theta}^2 + mx_0\Omega^2\cos(bq+\theta)]\mathrm{sign}(\dot{\theta}) \tag{8}$$

where c_0 is the modal damping coefficient of the primary structure, $f_0(\dot{q},t)$ denotes the turbulence induced modal load on the blade considering aerodynamic damping. Using the equations (3), (5), (6) and (8), the equations of motion of the blade-roller system can be obtained from the stationary conditions of the Euler-Lagrange equations:

$$\begin{aligned}&\left(m_0 + m_e(a^2 + R_e^2b^2)\right)\ddot{q} + m_eR_e^2b\ddot{\theta} + c_0\dot{q} + \left(k_0 - \Omega^2(m_0 + m_ea^2)\right)q + m_eR_e(2ab\dot{q} + a\ddot{\theta} - ab\Omega^2)\cos(bq+\theta)\\ &-m_eR_e\left((a - bx_0)\Omega^2 + 2a\Omega\dot{\theta} + a(b\dot{q} + \dot{\theta})\right)\sin(bq+\theta) - mg\left(a\sin(\Omega t) + bR_e\sin(\Omega t + bq + \theta)\right) = f_0(\dot{q},t)\end{aligned} \tag{9}$$

$$\begin{aligned}&m_eR_e^2b\ddot{q} + m_eR_e^2\ddot{\theta} + \mu_fR_e[mR_e\dot{\theta}^2 + mx_0\Omega^2\cos(bq+\theta)]\mathrm{sign}(\dot{\theta})\\ &+m_eR_ea(\ddot{q} - \Omega^2q)\cos(bq+\theta) + m_eR_e(2a\Omega\dot{q} + \Omega^2x_0)\sin(bq+\theta) - mgR_e\sin(\Omega t + bq + \theta) = 0\end{aligned} \tag{10}$$

Assuming small values of $q(t)$ and $\theta(t)$ and ignoring the influence of gravity, the angular natural frequency of the roller can be calculated from Equation (10) as:

$$\omega_d = \sqrt{\frac{m_eR_e\Omega^2x_0}{m_eR_e^2}} = \sqrt{\frac{x_0\Omega^2}{R_e}} \tag{11}$$

Defining $\chi = \omega_d/\omega_0$ as the frequency ratio between the damper and the structure, $\mu = m/m_0$ as the mass ratio between the damper and the 1st modal mass of the blade, the parameters of the roller damper to be optimized are χ and μ_f if x_0, Ω and μ are fixed.

2.2. TLCD

TLCD is a special type of the tuned liquid damper that relies on the motion of the liquid column in a U-shaped tube to counteract the action of external forces acting on the primary structure. Similar with the roller damper, by tuning the natural frequency of the liquid column to that of the 1st edgewise mode, the TLCD could effectively add damping into the system. As shown in Figure 2 (b), since the U-shaped tube is mounted inside a rotating blade with changing azimuthal angle, it should be manufactured in a closed form to prevent the liquid from leaking out of the tube. In this case, an extra

slim tube connecting two vertical tubes is fixed in order to balance the pressure above the liquid column during oscillation. L, B and H denote the overall length, the horizontal length and the vertical length of the liquid column, where $L=B+2H$, and A and A_0 denote the horizontal and vertical cross-sectional areas of the liquid column, respectively. The displacements of the liquid in the vertical column and the horizontal column are denoted $v(t)$ and $v_0(t)$, respectively. The continuity of liquid motion indicates that the liquid velocity in the vertical column and horizontal column has the relationship of $\dot{v}_0 = \alpha \dot{v}$, where $\alpha = A / A_0$ is the area ratio. The liquid mass is given as $m = \rho(2HA + BA_0)$, where ρ is the mass density of the liquid.

For ease of derivation, the following auxiliary parameters are introduced (see Figure 2 (b)):

$$\dot{v}_2(t) = -(x_0\Omega + a\dot{q})\cos(bq), \quad \dot{v}_3(t) = (x_0\Omega + a\dot{q})\sin(bq), \quad \kappa(t) = \Omega t + bq \tag{12}$$

where $\dot{v}_2(t)$ and $\dot{v}_3(t)$ denote the velocities of the center point O of the horizontal tube in y_2- and y_3-direction, respectively. $\kappa(t)$ is the rotational angle between the global X_3- and the local y_3- axis. Then, the potential and kinetic energy of the liquid column inside the tube can be given as:

$$\begin{aligned} U_d &= mg(x_0\cos\Psi - aq\sin\Psi) - \rho A v g\left(-\frac{1}{2}(2H - v)\cos\kappa - \frac{1}{2}B\sin\kappa\right) + \rho A v g\left(-\frac{1}{2}(2H + v)\cos\kappa + \frac{1}{2}B\sin\kappa\right) \\ &= mg(x_0\cos\Psi - aq\sin\Psi) + \rho A v g(-v\cos\kappa + B\sin\kappa) \end{aligned} \tag{13}$$

$$\begin{aligned} T_d &= \frac{1}{2}\rho A\int_{-(H-v)}^{0}\left((\dot{v}_2 - y_3\dot{\kappa})^2 + (\dot{v}_2 + \dot{v} - \frac{1}{2}(B-D)\dot{\kappa})^2\right)dy_3 \\ &\quad + \frac{1}{2}\rho A\int_{-(H+v)}^{0}\left((\dot{v}_2 - y_3\dot{\kappa})^2 + (\dot{v}_2 - \dot{v} + \frac{1}{2}(B-D)\dot{\kappa})^2\right)dy_3 + \frac{1}{2}\rho A_0\int_{-B/2}^{B/2}\left((\dot{v}_2 + \dot{v}_0)^2 + (\dot{v}_3 + y_2\dot{\kappa})^2\right)dy_3 \\ &= \rho A\left[(H^3 + 3Hv^2)\frac{\dot{\kappa}^2}{3} + (H^2 + v^2)\dot{\kappa}\dot{v}_2 + \frac{1}{4}H(4\dot{v}_2^2 + 4\dot{v}_3^2 + (2\dot{v} - B\dot{\kappa})^2) - v(2\dot{v} - B\dot{\kappa})\dot{v}_3\right] \\ &\quad + \frac{1}{24}\rho A_0 B\left(12(\dot{v}_0 + \dot{v}_2)^2 + 12\dot{v}_3^2 + B^2\dot{\kappa}^2\right) \end{aligned} \tag{14}$$

where g denotes the acceleration of gravity.

The inherent damping of the TLCD is introduced in the oscillating liquid column through an orifice, which is placed at the center of the horizontal tube (point O). The damping force of the liquid motion can be expressed as:

$$f_d(t) = \frac{1}{2}\xi\rho A_0|\dot{v}_0|\dot{v}_0 = \frac{1}{2}\xi\rho\alpha^2 A_0|\dot{v}|\dot{v} \tag{15}$$

where ξ is the head loss coefficient, a parameter controlled by the opening ratio of the orifice. Then, the two generalized loads for the degrees of freedom $q(t)$ and $v(t)$ are given by:

$$F_q(t) = f_0(\dot{q}, t) - c_0\dot{q}, \quad F_v(t) = -f_d(t) = -\frac{1}{2}\xi\rho\alpha^2 A_0|\dot{v}|\dot{v} \tag{16}$$

Using the equations (3), (13), (14) and (16), the equation of motion of the blade-TLCD system can be obtained from the stationary conditions of the Euler-Lagrange equations:

$$\begin{aligned} &m_4\ddot{q} + m_5\ddot{v} + c_0\dot{q} + 2m_6 v\dot{v} + m_7(2v\dot{v}\dot{q} + v^2\ddot{q}) + (k_0 - m_0\Omega^2)q + k_3 v\cos(\Omega t + bq) + k_4 v^2\sin(\Omega t + bq) - mga\sin(\Omega t) + \\ &\sin(bq)[-(bm_8 + m_{23}) - (bm_9 + m_{24})\dot{q} - (bm_{10} - m_{13} + m_{25})\dot{v} - (bm_{11} + m_{27})v^2 - m_{26}\dot{q}^2 + m_{15}\dot{v}^2 + \frac{1}{2}m_{14}\dot{v}\dot{q} + m_{14}v\ddot{q} + \\ &\quad m_{15}v\ddot{v} - (bm_{12} + m_{28})v^2\dot{q} - m_{29}v^2\dot{q}^2] + \\ &\cos(bq)[m_9\ddot{q} + m_{10}\ddot{v} + (bm_{13} - m_{19})v + (bm_{14} - m_{20})v\dot{q} + (2m_{11} + bm_{15} - m_{21})v\dot{v} + m_{12}v\dot{v}\dot{q} - m_{22}v\dot{q}^2 + m_{12}v^2\ddot{q}] = f_0(\dot{q}, t) \end{aligned} \tag{17}$$

$$\begin{aligned} &m_5\ddot{q}+m_{16}\ddot{v}+0.5\xi\rho\alpha^2A_0\left|\dot{v}\right|\dot{v}+(-m_{30})v-2m_6v\dot{q}-m_7v\dot{q}^2+k_5\sin(\Omega t+bq)+k_6v\cos(\Omega t+bq)+\\ &\sin(bq)[-(bm_{17}-m_{32})-(bm_{10}+m_{13})\dot{q}+(m_{18}-m_{19})\dot{v}-0.5m_{14}\dot{q}^2+m_{15}v\ddot{q}]+\\ &\cos(bq)[m_{10}\ddot{q}+(bm_{18}-m_{31})v+(bm_{15}-2m_{11})v\dot{q}-m_{12}v\dot{q}^2]=0 \end{aligned} \tag{18}$$

where the parameters m_4-m_{32} and k_3-k_6 are provided in Appendix A.

Assuming small values of $q(t)$ and $v(t)$ and ignoring the influence of gravity, the angular natural frequency of the liquid can be calculated from Equation (18) as:

$$\omega_d=\sqrt{\frac{-m_{30}-m_{31}}{m_{16}}}=\sqrt{\frac{2(x_0-H)\Omega^2}{2H+\alpha B}}=\sqrt{\frac{2x_0-(1-\gamma)L}{L+(\alpha-1)\gamma L}}\Omega \tag{19}$$

where $\gamma=B/L$ is the ratio of the horizontal length to overall length of the liquid column. Given x_0, Ω, α, γ and μ, the parameter of the TLCD to be optimized are χ and ξ. Then, L can be determined from equation (19), which in turn determines the value of B and H.

3. Numerical simulations

The NREL 5 MW baseline wind turbine [9] is utilized to calibrate the 2-DOF models. Each blade has a length of 63m and an overall mass of 17740 kg. The related data of the modal shape, the bending stiffness and mass per unit length of the blade can also be found in [9].

A 3-dimensional rotational sampled turbulence has been generated with given mean wind speed and turbulence intensity [8]. By applying this turbulence field to the rotor of the 13-DOF wind turbine model, we can obtain edgewise modal loads for each blade, based on which the optimization and parametric studies of the dampers are to be carried out. In the simulation, the fourth-order Runge-Kutta method was applied to solve the nonlinear ordinary differential equations of the 2-DOF models.

The reduction ratio η is defined as:

$$\eta=\frac{\sigma_{q,0}-\sigma_q}{\sigma_{q,0}} \tag{20}$$

where $\sigma_{q,0}$ and σ_q are the standard deviations of the edgewise tip displacements of the blade without and with control, determined as $\sigma_q=\left(\frac{1}{T}\int_0^T\left(q(t)-\mu_q\right)^2dt\right)^{\frac{1}{2}}$, where $\mu_q=\frac{1}{T}\int_0^T q(t)dt$ and T is the total sampling time. The optimal damper parameters can be found by maximizing the value of η.

3.1. Optimization and parametric study of the roller damper

The modal load is calculated from a turbulence field with a mean wind speed of 15 m/s and a turbulence intensity of 0.1. Since the control effect of the damper is dominated by the centrifugal acceleration $x_0\Omega^2$, it is expected that we can obtain better control effect by mounting the damper closer to the blade tip. On the other hand, the available space inside the blade is decreasing towards tip, which makes the determination of x_0 a practical tradeoff problem. In the following optimization procedure x_0 is set to be 45 m, 50 m and 55 m respectively. Moreover, it is well known that the larger mass ratio μ would give a better control performance for a passive damper. However, the damper mass should be limited according to the construction and maintenance considerations. Thus two sets of mass rations are considered, i.e. μ=3%, μ=4%. For each combination of the assigned value of x_0 and μ, we search for the optimal values of the tuning ratio χ and the friction coefficient μ_f by maximizing η, as shown in Table 1. Moreover, with the optimized damper parameters, the resulting maximum rotational angle of the roller θ_m, and the equivalent radius R_e are also calculated and presented in Table 1. Due to the restriction of space, we suggest to devise the tube in the form of an arc, of which the chord length C can be calculated as $C=2R_e\sin(\theta_m)$. The value of C can be regarded as the horizontal size of the roller damper.

From Table 1, there are four observations to be made: (i) the control effect increases as the mass ratio increases; (ii) a damper mounted closer to the tip can reduce the edgewise vibration more

efficiently; (iii) the optimal value of χ decreases as x_0 and μ increases, while the optimal value of μ_f does not change much when x_0 and μ changes; (iv) the maximum rotational angle of the roller reduces as x_0 and μ increases. However, the resulting chord length C is almost unchanged as long as μ is unchanged.

Table 1: Optimal parameters of the roller damper

μ=3% (m=42.36 kg)							μ=4% (m=56.48 kg)						
x_0 (m)	χ_{opt}	$\mu_{f,opt}$	η (%)	θ_m (rad)	R_e (m)	C (m)	x_0 (m)	χ_{opt}	$\mu_{f,opt}$	η (%)	θ_m (rad)	R_e (m)	C (m)
45	0.982	0.034	36.70	0.772	1.595	2.226	45	0.960	0.031	38.72	0.675	1.671	2.089
50	0.945	0.032	39.61	0.676	1.916	2.396	50	0.923	0.025	42.52	0.538	2.011	2.061
55	0.923	0.027	43.24	0.552	2.212	2.319	55	0.915	0.025	46.05	0.475	2.248	2.058

If the roller parameters shift away from their respective optimal values, the control effect is expected to degrade. It is observed that the detuning effect of χ is more pronounced when it shifts from the optimal value towards larger values and the damper is more robust in the frequency range of $0.9<\chi<1$ [8]. On the other hand, the reduction ratio is not so sensitive to the detuning of μ_f when μ_f is set to be larger than 0.02 [8].

3.2. Optimization and parametric study of the TLCD

More variables enter into the equations of motion of the blade-TLCD system than that of the blade-roller system. Hence we fix x_0=55 m in order to evaluate the influence of other parameters on the control effect. By assigning different values of μ, α and γ, the optimal frequency ratio, the optimal head loss coefficient can be determined, as shown in Table 2. It should be noted that the optimization has been carried out with the constraint that the maximum liquid response v_m should not exceed the vertical length of the liquid column H ($v_m/H\leq1$). This constraint is used so that the liquid of the TLCD remains in the vertical column all the time and the equations of motion of the blade-TLCD system are valid. With the optimal value of χ and ξ, the resulting values of the reduction ratio η, the ratio v_m/H and the horizontal length B are calculated and presented in Table 2. In all cases, the value of v_m/H is below 1, which ensures the validity of the equations of motion as well as the optimized parameters.

Table 2: Optimal parameters of the TLCD with constraint $v_m/H\leq1$ (x_0=55 m)

μ=3% (m=42.36 kg)							μ=4% (m=56.48 kg)						
α	γ	χ_{opt}	ξ_{opt}	η (%)	v_m/H	B (m)	α	γ	χ_{opt}	ξ_{opt}	η (%)	v_m/H	B (m)
	0.5	0.997	2	30.03%	0.969	1.860		0.5	0.99	2.4	32.07%	0.839	1.888
1	0.6	0.99	3.5	32.41%	0.999	2.273	1	0.6	0.982	3	35.03%	0.965	2.307
	0.7	0.99	9.5	31.14%	0.994	2.661		0.7	0.975	7.5	35.80%	0.992	2.743
	0.5	0.997	2	29.27%	0.903	1.493		0.5	0.99	1.9	31.63%	0.860	1.515
1.5	0.6	0.99	3.5	31.39%	0.952	1.754	1.5	0.6	0.982	2.5	34.60%	0.986	1.781
	0.7	0.99	8.5	30.59%	0.996	1.977		0.7	0.975	7	35.08%	0.993	2.373
	0.5	0.997	1.5	28.74%	0.983	1.247		0.5	0.99	1.6	30.91%	0.895	1.247
2	0.6	0.99	3	30.70%	0.988	1.428	2	0.6	0.982	2.5	33.81%	0.981	1.450
	0.7	0.99	8.5	29.30%	0.983	1.572		0.7	0.975	7	33.86%	0.982	1.620

From Table 2, there are six observations to be made: (i) as μ increases, the control effect increases and the value of v_m/H reduces; (ii) the optimal value of χ decreases as μ and γ increases, but the variation of α has no effect on χ_{opt}; (iii) the optimal value of ξ increases as γ increases in order to limit the value of v_m/H. The variations of α *and* μ have no clear effect on ξ_{opt}; (iv) for μ=4%, the increase of γ increase the control effect of the TLCD since the mass of the horizontal part of TLCD is the only effective mass acting on the structure; (v) as the mass ratio reduces to 3%, η does not increase monotonously with γ due to the constraint of $v_m/H\leq1$. For example, in the cases of γ=0.7, the values of ξ_{opt} are larger than their counterparts when μ=4%, so that the constraint of $v_m/H\leq1$ is fulfilled, resulting in the fact that η is even smaller comparing with the reduction of γ=0.6; (vi) the increase of α reduces the total length L of the liquid column as well as the horizontal length B, but reduces the control effect of the TLCD slightly.

3.3. Comparison between the roller damper and the TLCD

Based on the results in Table 1 and 2, comparisons on the control efficiency of the roller damper and the TLCD can be carried out in the case of x_0=55 m. For a given mass ratio, the control performance of the roller damper is always better than that of the TLCD. For μ=3%, the maximum reduction coefficient η is increased from 32.41% (for TLCD) to 43.24% (for roller damper), while for μ=4%, the maximum reduction coefficient is increased from 35.80% (for TLCD) to 46.05% (for roller damper). The reason is that the effective mass of the roller damper is $m_e = (7/5)m > m$ [8], while the effective mass of the TLCD is $m_e = (B/L)m < m$.

Figure 3 presents the comparison of the edgewise vibration without control, with a TLCD and with a roller damper, where the optimized damper parameters are used. Same time series of the modal load has been used in the three cases in order to make a meaningful comparison. It is observed from the time histories in Figure 3 (a) that both the TLCD and the roller damper significantly suppress the edgewise vibrations, and that the roller damper obtains somewhat better control performance than the TLCD. The Fourier amplitude spectrum of $q(t)$ as illustrated in Figure 3 (b) shows that both dampers effectively suppress the peak around 6.85 rad/s corresponding to the eigenvibration of the blade in edgewise direction, and this peak is slightly lower when the roller damper is utilized. This means a properly tuned roller damper or TLCD could almost totally absorb energy from the eigenvibration of the blade. Further, it is noted that all frequencies below 6.85 rad/s are hardly affected by the dampers, including a low peak around 1.267 rad/s. This peak is associated with the rotational speed of the blade, and both the dampers are not functioning at this frequency. It should be noted that much more energy is concentrated around the frequency of 6.85 rad/s for the uncontrolled response since aerodynamic damping is low in the edgewise direction. As a result, although not functioning around the frequency of Ω, a well-tuned TLCD or roller damper still exhibit promising performance in suppressing edgewise vibrations.

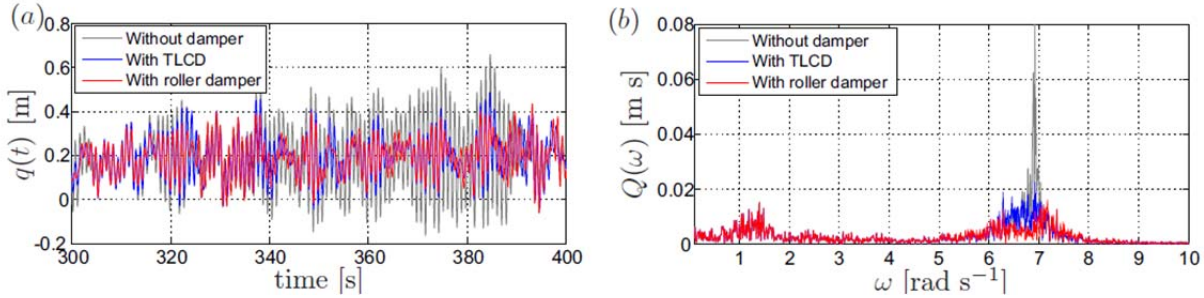

Figure 3: Blade edgewise vibrations without damper, with TLCD and with roller damper, V_0=15 m/s, I=0.1, μ=3%, x_0=55 m. (a) Time series, (b) Fourier amplitude.

Although the control performance of the roller damper is always better than the TLCD, there may well be other practical situations when the latter type is still preferred. In the case of x_0=55 m, the horizontal length (C) of the roller damper is 2.319 m for μ=3% and 2.058 m for μ=3%, which may make it impossible to install the damper inside that part of the blade. Since the size of the roller damper cannot be further reduced as long as χ is fixed, the only solution is to mount the damper further away from tip, where more space is available. On the other hand, the size of the TLCD can be adjusted easily by changing the value of α and γ. For example, the maximum reduction coefficient of the TLCD (32.41%) is obtained when α=1 and γ=0.6, which result in an unacceptable horizontal length B=2.273 m. However, by increasing α to 1.5 and keeping γ unchanged, the value of B is reduced to 1.754 m while the control effect is very slightly affected. Moreover, the damping effect of TLCDs is easier to quantify by changing the opening ratio of the orifice, while it is difficult to accurately quantize the friction coefficient between the roller and the tube. This means the performance prediction of TLCDs could be more accurate than that of the roller damper, when applying the dampers into practical project.

3.4. Evaluation by the 13-DOF aeroelastic wind turbine model

To verify the applicability of the decoupled optimization and the control effect of the dampers in highly coupled wind turbine systems, the optimized dampers are incorporated into a 13-DOF aeroelastic model, as illustrated in Figure 4. The details of the 13-DOF model are described in [8], and it takes several important characteristics of a wind turbine into account, including time dependent system matrices, coupling of the tower-blades-drivetrain vibrations as well as nonlinear aeroelasticiy. For each blade a roller damper or a TLCD is mountd at the position of x_0=55 m. Therefore, a 16-DOF system is obtained for the wind turbine with a roller damper or a TLCD mounted in each blade.

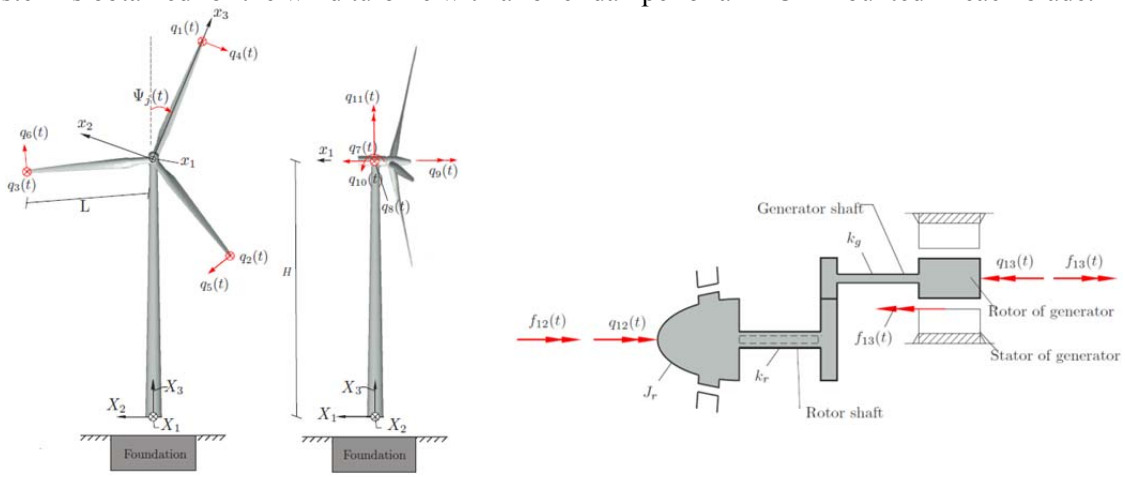

Figure 4: 13-DOF aeroelastic model of three bladed wind turbine. Definition of fixed and moving frames of reference and the degrees of freedom.

Figure 5 shows the edgewise vibration in blade 1, with the same damper parameters and the same turbulence field as used for Figure 3. It is shown from Figure 5 (a) that both the optimized roller damper and TLCD effectively mitigate edgewise vibrations. The standard deviation is reduced by 25.63% (the TLCD) and 36.57% (the roller damper), respectively. Similar with the results in Figure 3, the roller damper is more effective than the TLCD. Figure 5 (b) shows that the frequency component corresponding to eigenvibration of the blade is significantly reduced by the roller damper and the TLCD, and this peak is lower when the roller damper is utilized. Comparing with the results obtained from the 2-DOF models, the control effects of both dampers are slightly reduced when incorporated into the highly coupled 13-DOF model. This is because the couplings of the blade edgewise vibration to other degrees of freedom cause a transfer of mechanical energy from the edgewise vibration to other vibrational modes, resulting in a reduced mitigation efficiency of the dampers. Nevertheless, the roller damper and the TLCD with parameters optimized from the reduced 2-DOF models still achieve promising performance on the highly coupled 13-DOF model.

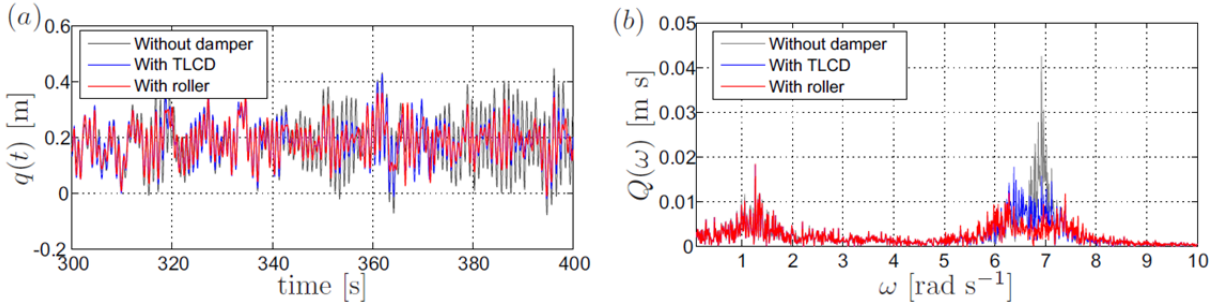

Figure 5: Blade edgewise vibrations without damper, with TLCD and with roller damper, obtained from the 16-DOF system. V_0=15 m/s, I=0.1, μ=3%, x_0=55 m. (a) Time series, (b) Fourier amplitude.

4. Conclusions

The present paper investigates the effectiveness of roller dampers and TLCDs in mitigating edgewise vibrations in wind turbine blades. Parametric optimizations of the dampers have been carried out using the decoupled 2-DOF nonlinear models developed for a rotating blade equipped with a roller damper or a TLCD. More variables need to be considered in the optimization procedure of TLCDs, making the design of TLCDs more flexible in different application problems. The simulation results show that roller dampers are more effective in suppressing edgewise vibrations than TLCDs for a given mass ratio, because the roller damper has a larger effective mass than that of the TLCD. On the other hand, TLCDs offer some unique practical advantages, such as accurate quantification of damping property, flexible installation, easy adjustment and almost maintenance free. Both roller dampers and TLCDs are promising to be utilized in wind turbine blades for edgewise vibration control.

The problems to be further studied include (1) the detuning effect on the control performance when the TLCD parameters shift away from the optimal values; (2) experimental validation of the performance of both the roller damper and the TLCD.

Acknowledgements
The first author gratefully acknowledges the financial support from the Chinese Scholarship Council under the State Scholarship Fund.

Appendix A

$$
\begin{aligned}
&m_4 = m_0 + \frac{2}{3}\rho A b^2 H^3 + \frac{1}{2}\rho AH(4a^2 + b^2B^2) + \frac{1}{12}\rho A_0 B(12a^2 + b^2B^2),\ \ m_5 = -\rho ABHb,\ \ m_6 = 2\rho AHb\Omega \\
&m_7 = 2\rho AHb^2,\ m_8 = -\rho A(a + bx_0)H^2\Omega,\ m_9 = -2\rho AabH^2,\ m_{10} = -\rho AaB,\ m_{11} = -\rho A(a + bx_0)\Omega \\
&m_{12} = -2\rho Aab,\ m_{13} = \rho A(a + bx_0)B\Omega,\ m_{14} = 2\rho AabB,\ m_{15} = -2\rho Aa,\ m_{16} = \rho A(2H + \alpha B) \\
&m_{17} = -\rho AB\Omega x_0,\ m_{18} = -2\rho A\Omega x_0,\ m_{19} = \rho ABbx_0\Omega^2,\ m_{20} = \rho ABb(a + bx_0)\Omega,\ m_{21} = -2\rho Abx_0\Omega \\
&m_{22} = \rho ABab^2,\ m_{23} = \rho AH^2bx_0\Omega^2,\ m_{24} = \rho AbH^2(a + bx_0)\Omega^2,\ m_{25} = \rho ABbx_0\Omega,\ m_{26} = \rho AH^2ab^2 \\
&m_{27} = \rho Abx_0\Omega^2,\ m_{28} = \rho Ab(a + bx_0)\Omega,\ m_{29} = \rho Aab^2,\ m_{30} = 2\rho AH\Omega^2,\ m_{31} = -2\rho Ax_0\Omega^2 \\
&m_{32} = \rho ABx_0\Omega^2,\ k_3 = \rho AgBb,\ k_4 = \rho Agb,\ k_5 = \rho AgB,\ k_6 = -2\rho Ag
\end{aligned}
\tag{21}
$$

References

[1] Hansen M H 2007 Aeroelastic instability problems for wind turbines *Wind Energy*. **10** 551-577
[2] Murtagh P J, Ghosh A, Basu B and Broderick B M 2008 Passive control of wind turbine vibrations including blade/tower interaction and rotationally sampled turbulence *Wind Energy*. **11** 305-317
[3] Colwell S and Basu B 2009 Tuned liquid column dampers in offshore wind turbines for structural control *Eng. Sturct.* **31** 358-368
[4] Zhang Z L, Chen J B and Li J 2013 Theoretical study and experimental verification of vibration control of offshore wind turbines by a ball vibration absorber *Struct. Infrastruct. Eng.* (preprint 10.1080/15732479.2013.792098)
[5] Fitzgerald B, Basu B and Nielsen S R K 2013 Active tuned mass dampers for control of in-plane vibrations of wind turbine blades *Struct. Control. Health Monit*. **20** 1377-1396
[6] Krenk S, Svendsen M N and Høgsberg J 2012 Resonant vibration control of three-bladed wind turbine rotors *AIAA J.* **50** 148-161
[7] Staino A, Basu B and Nielsen S R K 2012 Actuator control of edgewise vibrations in wind turbine blades *J. Sound Vibr.* **331** 1233-1256
[8] Zhang Z, Li J, Nielsen S R K and Basu B 2014 Mitigation of edgewise vibrations in wind turbine blades by means of roller dampers *J. Sound Vibr.* (submitted)
[9] Jonkman J, Butterfield S, Musial W and Scott G 2009 Definition of 5-MW reference wind turbine for offshore system development *Technical Report NREL/TP-500-38060*.